

Probe the tilted Quark-Gluon Plasma with charmonium directed flow

Baoyi Chen,^{1,*} Maoxin Hu,¹ Huanyu Zhang,¹ and Jiaxing Zhao^{2,†}

¹*Department of Physics, Tianjin University, Tianjin 300350, China*

²*Department of Physics, Tsinghua University, Beijing 100084, China*

(Dated: January 22, 2022)

Charmonium directed flows are studied based on transport model coupled with the realistic three dimensional expansions of the bulk medium. The non-central symmetric nucleus-nucleus collisions can generate the rotating quark-gluon plasma (QGP) with symmetry-breaking longitudinal distributions. In $\sqrt{s_{NN}} = 200$ GeV Au+Au semi-central collisions, charmonium are primordially produced in the initial hard process, they are mainly dissociated by the initial tilted source with high temperatures and then move out of the bulk medium to keep the early information of the medium. The momentum distribution of primordially produced charmonia is less affected by the hydrodynamic expansions of QGP where its tilted shape is being diluted. This biased dissociation can generate directed flows of J/ψ and $\psi(2S)$ which are much larger than the values of light charged hadrons and open heavy flavor. Charmonium directed flows can help to quantify the rapidity-odd distributions of QGP initial energy densities in nucleus-nucleus collisions.

PACS numbers: 25.75.-q, 12.38.Mh, 14.40.Lb

It's well known that a strong electromagnetic field and a strong vorticity field can be generated in the non-central relativistic heavy ion collisions. Due to the coupling between the parton spin and vorticity field, some interesting effects about the polarizations of quarks and hadrons have been studied [1–3]. Theoretical and experimental studies show that the light charged hadrons [4–6] and open heavy flavor such as D-mesons [7, 8] carry non-zero directed flows from the anisotropic expansions of the bulk medium. The magnitudes of these effects induced by the vorticity field depend sensitively on the rotations of initial QGP in semi-central nucleus-nucleus (AA) collisions. The evolutions of rotating QGP can be simulated by the hydrodynamic model. The initial energy density of QGP produced in the relativistic heavy ion collisions can be extracted with other models and constrained by the final distributions of charged particles. Directed flows of charged particles and D mesons in experiments indicate the rapidity-odd energy density of QGP in the longitudinal direction. This tilted magnitude of the energy density will be diluted by the hydrodynamic expansions. Different from light partons, heavy quarks are produced in parton hard scatterings, and symmetrically distributed in forward-backward rapidities at the moment of nuclear collisions. In forward and backward rapidities of the tilted medium, heavy quarks and quarkonium undergo different number of elastic(inelastic) collisions with the bulk medium when moving in the different directions in the transverse plane. This results in the final anisotropic momentum distribution of heavy flavors in the transverse plane, such as directed flow v_1 , elliptic flow v_2 , etc. For open heavy flavors, their dragged movement by the QGP expansion also contributes to the

anisotropic flows of charm quarks [4, 7]. The large uncertainty of heavy quark diffusion coefficient prevents further solid conclusions about D-meson directed flow [9].

Charmonium as a bound state is first proposed to be a probe of the deconfined phase in the early stage of relativistic heavy ion collisions [10]. They are mostly dissociated in the initial stage where medium temperature is high. In the later stage of QGP hydrodynamic expansions, charmonium momentum distribution is not effectively changed by the elastic scatterings with light partons because of charmonium large mass and zero color charge. This makes charmonium a relatively clean probe for the initial anisotropic deposition of the bulk medium. Primordial charmonia are produced symmetrically in forward-backward rapidity with isotropic transverse momentum distribution in Au+Au collisions. After experiencing biased dissociations in tilted source, the rapidity-odd distributions and transverse elliptic distributions of the initial QGP result in the directed and elliptic flows of charmonia respectively. These observables help to constrain the magnitude of the tilt in the longitudinal deposition of initial energy density in Au+Au collisions.

Charmonium evolution in the hot medium has been widely studied with rate equation [11, 12] and transport model [13–15]. From the lattice QCD calculations, heavy quarkonium potential is partially screened by the deconfined medium. Charmonium bound states can also be dissociated through the inelastic scatterings with partons. Both of these hot medium effects suppress the charmonium final yields, and can be included in the transport equation,

$$\partial_t f_\psi(\mathbf{x}, \mathbf{p}, t) + \mathbf{v} \cdot \nabla f_\psi(\mathbf{x}, \mathbf{p}, t) = -\alpha_\psi(\mathbf{p}, T) f_\psi(\mathbf{x}, \mathbf{p}, t) + \beta_\psi(\mathbf{p}, T) \quad (1)$$

where $\mathbf{v} = \mathbf{p}/E$ is the charmonium velocity. T is the QGP local temperature depending on coordinates and time. Charmonium density in phase space $f_\psi(\mathbf{x}, \mathbf{p}, t)$

*Electronic address: baoyi.chen@tju.edu.cn

†Electronic address: zhao-jx15@mails.tsinghua.edu.cn

changes with the time and coordinate due to their motions. f_ψ can also be affected by hot medium effects labelled as α_ψ and β_ψ terms on the right hand side of Eq.(1). α_ψ is charmonium dissociation rate in the QGP, the formula can be written as [13],

$$\alpha_\psi(\mathbf{p}, T) = \frac{1}{E_T} \int \frac{d^3\mathbf{k}}{(2\pi)^3 E_g} \sigma_{g\psi}(\mathbf{p}, \mathbf{k}, T) F_{g\psi}(\mathbf{p}, \mathbf{k}) f_g(\mathbf{k}, T) \quad (2)$$

where $E_T = \sqrt{m_\psi^2 + p_T^2}$ is the transverse energy, \mathbf{k} and E_g is the gluon momentum and energy. $F_{g\psi}$ is the flux factor. The dissociation rate is proportional to gluon density f_g and inelastic cross section $\sigma_{g\psi}$ between gluon and charmonium. The form of inelastic cross section for charmonium ground state J/ψ in vacuum is calculated with the method of operator production expansion [16]. Its value at finite temperature is obtained by reducing its binding energy in the formula to consider the color screening effect [17]. The inelastic cross section for excited state ($\chi_c, \psi(2S)$) is obtained by the geometry scale with the ground state J/ψ , please see the details in Ref.[18]. Meanwhile, within the deconfined phase, uncorrelated charm pairs produced in the hard process of initial hadronic collisions evolve randomly. They may recombine into a new bound state [19, 20], labelled with β_ψ in Eq.(1). The regeneration term depends on the densities of charm and anti-charm quarks and their combination probability into a charmonium state [21]. The regeneration contribution is suppressed in the non-central AA collisions at the RHIC energy due to the small density of charm pairs in QGP in these collisions [22, 23]. Therefore, we neglect the regeneration contribution in this work.

Charmonium primordial distribution in AA collisions can be obtained from the distribution in pp collisions with the modification of cold nuclear matter effect [24–28]. The primordial distribution in the transverse plane in AA collisions is written as [29],

$$f_{t=0}(\mathbf{x}_T, \mathbf{p}_T, y_p | \mathbf{b}) = T_A(\mathbf{x}_T^A) T_B(\mathbf{x}_T^B) \frac{d^2\sigma_{J/\psi}^{pp}}{dy_p 2\pi p_T dp_T} \times \mathcal{R}_{AB} \quad (3)$$

where $\mathbf{x}_T^A = \mathbf{x}_T + \frac{\mathbf{b}}{2}$ and $\mathbf{x}_T^B = \mathbf{x}_T - \frac{\mathbf{b}}{2}$. The centers of two nuclei are located at $\mathbf{x}_T = (\pm b/2, 0)$. $T_A(\mathbf{x}_T) = \int_{-\infty}^{+\infty} dz_A \rho_A(\mathbf{x}, z_A)$ is the thickness function of nucleus A(B). Nuclear density ρ_A is taken as Woods-Saxon distribution. \mathcal{R}_{AB} is the modification factor from cold nuclear matter effect. We employ the EPS09 NLO model to parameterize the homogeneous shadowing factor for charmonium in the entire regions of p_T and rapidity [30], and take the value $\mathcal{R}_{AB} = 0.85$ in $\sqrt{s_{NN}} = 200$ GeV Au+Au collisions. The shadowing effect is relatively weak at the RHIC colliding energy compared with the LHC colliding energies. It shows clear rapidity dependence in d+Au collisions, but tends to be flat with rapidity in symmetric AA collisions [31]. As we employ the homogeneous

factor for the shadowing effect, \mathcal{R}_{AB} suppress the charmonium nuclear modification factor and does not affect the final momentum anisotropies according to their definitions. The detailed p_T -dependence in \mathcal{R}_{AB} does not significantly change the p_T -integrated v_1 and v_2 . Charmonium anisotropic flows are mainly generated by the interactions with the hot medium in AA collisions. The differential cross section in pp collisions as a function of transverse momentum p_T and rapidity y_p is parametrized from the experimental data with the formula,

$$\frac{d^2\sigma_{J/\psi}^{pp}}{dy_p 2\pi p_T dp_T} = \frac{(n-1)}{\pi(n-2)\langle p_T^2 \rangle} \left[1 + \frac{p_T^2}{(n-2)\langle p_T^2 \rangle} \right]^{-n} \frac{d\sigma_{J/\psi}^{pp}}{dy_p} \quad (4)$$

$$\frac{d\sigma_{J/\psi}^{pp}}{dy_p} = A e^{-B y_p^2 \cosh(C y_p)} \quad (5)$$

with $n = 6.0$, mean squared transverse momentum in the central rapidity is taken from the experimental data $\langle p_T^2 \rangle|_{y_p=0} = 4.14$ (GeV/c)² [32], its rapidity dependence is fitted with $\langle p_T^2 \rangle = \langle p_T^2 \rangle|_{y_p=0} \times [1 - (y_p/y_{pmax})^2]$ with the charmonium maximum rapidity defined as $y_{pmax} = \cosh^{-1}(\sqrt{s_{NN}}/(2E_T))$ in pp collisions. Parameters in the rapidity dependence of charmonium cross section is fitted to be $A = 0.75$ μb , $B = 0.61$, $C = 1.2$ with the data in forward rapidities [31, 32]. Initial distributions of charmonium excited states are scaled from J/ψ distribution with a factor measured in pp collisions. As nucleus is accelerated to the speed of $v_N \sim 0.9999c$, nuclear shape is strongly Lorentz contracted in the longitudinal direction, charmonium primordial longitudinal distribution is simplified as $f_{t=0}(\mathbf{x}_T, z, \mathbf{p}_T, y_p | \mathbf{b}) = f_{t=0}(\mathbf{x}_T, \mathbf{p}_T, y_p | \mathbf{b}) \delta(z)$. After nuclear collisions, QGP needs a period of time $\tau_0 \sim 0.6$ fm/c to reach local equilibrium and to start transverse expansion. Both hydrodynamic models and transport equation Eq.(1) start from τ_0 . Before this time scale, charmonium is free streaming in the QGP pre-equilibrium stage. With primordial charmonia produced at the very beginning of nuclear collisions, their dissociations mainly happen in the early stage of QGP which makes them sensitive to the initial anisotropic distribution of QGP energy densities.

In order to calculate the charmonium directed and elliptic flows, one needs to generate realistic QGP evolutions at $\sqrt{s_{NN}} = 200$ GeV Au+Au collisions. When two nuclei collide with each other, the nucleus moving with the positive (negative) rapidity tends to tilt the produced bulk medium to positive (negative) x with respect to the beam axis for positive (negative) z . To explain the rapidity spectra of charged particles in Au+Au collisions, the initial tilted entropy density $s(\tau_0, \mathbf{x}_T, \eta_{||})$ is parametrized with [5, 8],

$$s(\tau_0, \mathbf{x}_T, \eta_{||}) = s_0 \times \exp[-\theta(|\eta_{||}| - \eta_{||}^0) \frac{(|\eta_{||}| - \eta_{||}^0)^2}{2\sigma^2}] \times [c_{hard} N_{coll} + (1 - c_{hard})(N_{part}^+ \zeta_+(\eta_{||}) + N_{part}^- \zeta_-(\eta_{||}))] \quad (6)$$

where s_0 and the exponential term represent initial entropy density and the rapidity distribution to reproduce the rapidity spectra of charged particles in AA collisions. N_{part}^+ and N_{part}^- is the number of participants in the forward and backward rapidities respectively. N_{coll} is the number of binary collisions. The initial entropy density comes from both soft (N_{part} terms) and hard (N_{coll} terms) collision process with a fraction $1 - c_{hard}$ and c_{hard} respectively. The parameters are fixed to be $c_{hard} = 0.05$, $\eta_{||}^0 = 1.0$, $\sigma = 1.3$. The specific rapidity-odd distribution in entropy is introduced by the function $\zeta_{\pm}(\eta_{||})$. It's taken as $\zeta_{\pm}(\eta_{||}) = \frac{\eta_T \pm \eta_{||}}{2\eta_T}$ at $|\eta_{||}| \leq \eta_T$. For $|\eta_{||}| > \eta_T$, they are fixed to their values at $\pm\eta_T$. η_T controls the magnitude of the tilt of the initial QGP and is taken as $\eta_T = 3.36$ [8]. Different values of parameter η_T will be taken, to provide different tilted backgrounds for charmonium evolutions. QGP initial energy distribution is plotted in Fig.1. One can clearly see the tilt of bulk medium distribution in forward and backward rapidities, which will result in biased dissociations and directed flows for charmonia. QGP expansions are simulated with (3+1)D hydrodynamic model (MUSIC) followed by the crossover phase transition to the hadronic phase [33, 34]. Its equation of state is obtained with the interpolation between lattice data and a hadron resonance gas [35]. In this work, hadron phase contribution on charmonium dissociation is neglected for simplicity.

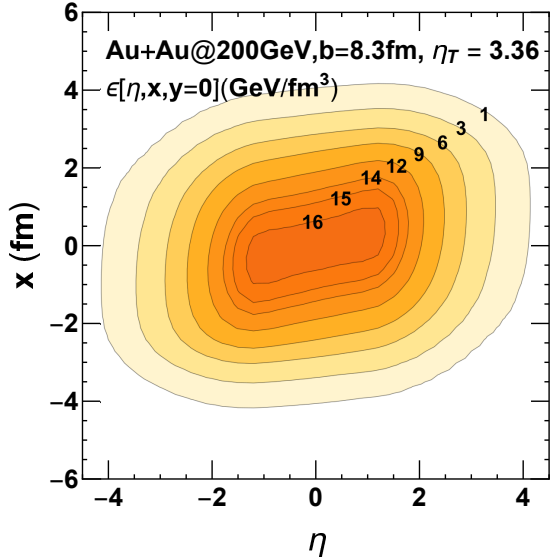


FIG. 1: (Color online) Spatial distributions of QGP initial energy density in the $x-\eta$ plane in $\sqrt{s_{NN}} = 200$ GeV Au+Au collisions with the impact parameter $b = 8.3$ fm. The transverse coordinate is chosen as $\mathbf{x}_T = (x, 0)$. The parameter for the QGP tilted magnitude is taken as $\eta_T = 3.36$. Different colors in the figure represent different values (1 ~ 16 GeV/fm³) of the QGP energy density.

Different from soft collisions, binary collision profiles are symmetric in forward and backward rapidities. Charmonium initial production from hard collisions is not

tilted. Therefore, its distribution is shifted relative to the tilted bulk medium. As the tilted shape of the medium is more obvious in the early stage of QGP evolutions where charmonium dissociation effect is the strongest, charmonium bound states are sensitive to the early information of QGP compared with the observables such as light hadrons or open heavy flavors. The nuclear modification factors R_{AA} of J/ψ and $\psi(2S)$ based on this framework have been extensively studied and compared with the experimental data in Ref.[18, 36].

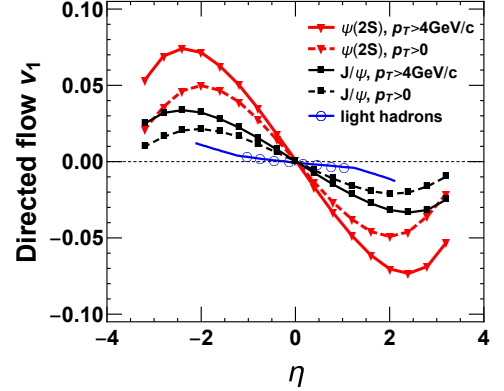


FIG. 2: (Color online) J/ψ and $\psi(2S)$ directed flows as a function of η in $\sqrt{s_{NN}} = 200$ GeV Au+Au collisions. Charmonium p_T range is integrated in $p_T > 0$ and $p_T > 4$ GeV/c respectively with dashed and solid lines. Impact parameter is taken as $b = 8.3$ fm for the centrality 0-80%. Charged hadron directed flow is also included for comparison: theoretical calculation with hydrodynamic model is cited from Ref.[8], experimental data is from STAR measurements [37]. The parameter for the QGP tilted magnitude is taken as $\eta_T = 3.36$.

In Fig.2, charmonium directed flows integrated in different p_T regions are compared with the charged particles. The impact parameter is set with $b = 8.3$ fm for the centrality 0-80%. In the figure, both J/ψ (thin black line) and $\psi(2S)$ (thick red line) directed flows are several times larger than the value of charged particles measured by STAR, because charmonia are directly dissociated by the asymmetric source in the early stage where the tilt is the largest. Excited state $\psi(2S)$ with smaller binding energy is easier to be dissociated in QGP due to the larger $\sigma_{g\psi(2S)}$, compared with the ground state J/ψ . $\psi(2S)$ directed flow is larger than the v_1 of J/ψ and charged particles. Note that even though the directed flows of both charmonia and charged hadrons are due to the tilted source in semi-central AA collisions, their processes are different. For charged particles and D mesons, their directed flows are mainly from the drag of tilted bulk medium with hydrodynamic expansions [8]. Charmonium directed flows are dominated by the biased dissociations due to the difference of their path lengths in the QGP initial stage. In the later stage of QGP expansions, charmonium momentum distribution is less affected by the elastic collisions with QGP. For the lines with $p_T > 0$ in Fig.2, charmonium directed flows are smaller. As char-

monium with smaller transverse velocity will stay longer inside the QGP. Hydrodynamic expansions will reduce the tilt of QGP, which makes charmonium biased dissociations not so obvious. For those charmonium with large momentum, they experience the initial tilted QGP and move out of the bulk medium quickly to keep the early information of the tilted source. Charmonium v_1 can be enhanced by around 50% when p_T range is shifted from $p_T > 0$ to $p_T > 4$ GeV/c.

To show that charmonia with larger p_T can keep more early information of the tilted source, we plot charmonium $v_1(p_T)$ in Fig.3. The magnitude of charmonium v_1 increases with p_T . This is consistent with Fig.2. As charmonia suffers different dissociations in positive- and negative- x -direction from the initial QGP due to the path-length-difference, and move out of the medium quickly, this makes charmonium $|v_1|$ and v_2 increase with p_T . This effect saturates at high p_T and does not drop to zero, please see Fig.3. The momentum anisotropy induced by this path-length-difference mechanism is different from the situations of light hadrons or D mesons which momentum anisotropies come from the QGP anisotropic expansion and usually satisfy the mass ordering: particles with smaller mass are easier to reach kinetic equilibrium with QGP expansion and carry larger collective flows.

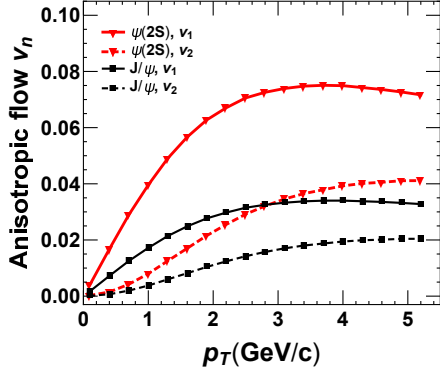


FIG. 3: (Color online) Directed and elliptic flows of J/ψ and $\psi(2S)$ as a function of transverse momentum p_T with the fixed rapidity $\eta = -2.4$, in $\sqrt{s_{NN}} = 200$ GeV Au+Au collisions. Other parameters are the same with Fig.2.

The external fields such as electromagnetic fields can also contribute to the directed and elliptic flows of open charm quarks. However, J/ψ and $\psi(2S)$ as a bound state of $c\bar{c}$ dipole, carry zero net electric and color charges. Its evolutions is less affected by the external fields, act as a relatively clean probe for the initial asymmetric distributions of the bulk medium in longitudinal direction and the transverse plane.

In order to check the charmonium directed flows with different tilted QGP, the parameter for the tilt in initial longitudinal distribution of energy density is shifted to be $\eta_T = 2$ (for larger tilted medium) and $\eta_T = 4$ (for smaller tilted medium). Both J/ψ and $\psi(2S)$ directed

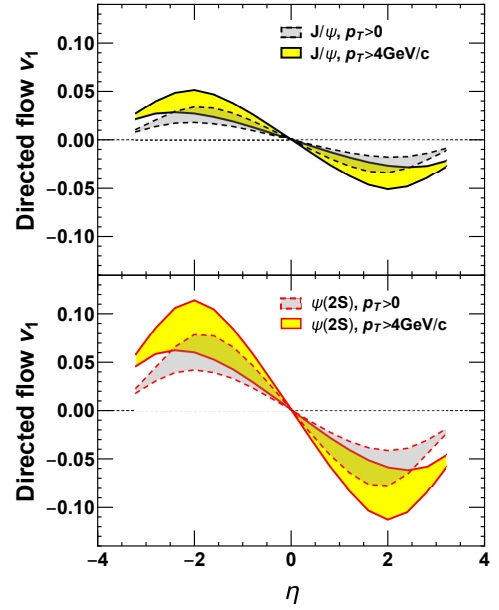


FIG. 4: (Color online) J/ψ (upper panel) and $\psi(2S)$ (lower panel) directed flows as a function of rapidity η with the p_T range $p_T > 0$ and $p_T > 4$ GeV/c respectively. Upper and lower limits of the bands corresponds to $\eta_T = 2$ and $\eta_T = 4$ respectively, which is the parameter for the tilt of the initial QGP. Other parameters are the same with Fig.2.

flows are presented in Fig.4. Their directed flows in high p_T bin is more sensitive to the tilted effect. In the forward and backward rapidity $|\eta| \sim 2$, prompt J/ψ and prompt $\psi(2S)$ directed flows can reach 0.05 and 0.11 respectively at $p_T > 4$ GeV/c, which are much larger than the situations of light charged hadrons $v_1^{\text{charged}} \sim 0.005$. In the medium with symmetric longitudinal distribution, charmonium directed flows drops to zero. With the QGP initial conditions given in Fig.1, charmonium directed flows from Fig.2 are close to the lower limits of the bands in Fig.4. These clear signals of charmonium directed flows are the promising probes for the QGP initial tilted distribution in forward-backward rapidity in AA collisions. Confirming and measuring the charmonium directed flows can help to determine the magnitude of the tilt in initial QGP. In Fig.1-4, Charmonium theoretical results are in the centrality 0-80% with impact parameter $b = 8.3$ fm. In other centralities, the tilt of QGP initial energy density and the value of η_T changes with the colliding centrality. For example, in the most central collisions with $b=0$, the tilt of QGP will disappear. In higher colliding energies such as LHC, most charmonia are from the regeneration instead of the initial production. The uncertainty of charm quark kinetic thermalization in the expanding QGP makes directed flows of regenerated charmonia ambiguous. The tilt of QGP initial energy density in LHC Pb-Pb collisions is also smaller than the situation in RHIC Au-Au collisions. Therefore, charmonium directed flows have a better chance to be

measured at RHIC energies than the LHC energies. However, with the limited data about charmonium currently available at RHIC energies, the p_T -integrated J/ψ observables in Fig.2 seems to be more prospective.

In this work, we have applied the transport model to study charmonium directed flows in the tilted QGP with the symmetry-breaking longitudinal distribution produced in semi-central Au+Au collisions at $\sqrt{s_{NN}} = 200$ GeV. In this centrality, charmonium production are dominated by the process of parton hard scatterings before the formation of QGP. In the early stage of QGP evolutions where its tilted shape is more clear, charmonium suffers stronger dissociations in the bulk medium with high temperatures. They experience biased dissociations due to the path-length-difference inside QGP in the transverse plane to obtain directed flows, and move quickly out of the bulk medium to keep the early information of the initial tilted source. This makes J/ψ

and $\psi(2S)$ directed flows several times larger than the charged hadrons. The median values of J/ψ and $\psi(2S)$ directed flows in $p_T > 4$ GeV/c can reach 0.03 and 0.07 in the backward rapidity, which are around 50% larger than the situation in $p_T > 0$. The development of charmonium v_1 from the path-length-difference is different from the situations of light hadrons or D mesons which come from QGP anisotropic expansions and usually satisfy the mass ordering. The signal of charmonium v_1 can help to extract the early asymmetric deposition of QGP energy density in the forward-backward rapidity in symmetric AA collisions.

Acknowledgement: This work is supported by NSFC Grant No. 11705125 and Sino-Germany (CSC-DAAD) Postdoc Scholarship.

-
- [1] Z. T. Liang and X. N. Wang, Phys. Rev. Lett. **94**, 102301 (2005) Erratum: [Phys. Rev. Lett. **96**, 039901 (2006)]
 - [2] L. G. Pang, H. Petersen, Q. Wang and X. N. Wang, Phys. Rev. Lett. **117**, no. 19, 192301 (2016)
 - [3] F. Becattini *et al.*, Eur. Phys. J. C **75**, no. 9, 406 (2015) Erratum: [Eur. Phys. J. C **78**, no. 5, 354 (2018)].
 - [4] L. Adamczyk *et al.* [STAR Collaboration], Phys. Rev. Lett. **112**, no. 16, 162301 (2014)
 - [5] P. Bozek and I. Wyskiel, Phys. Rev. C **81**, 054902 (2010).
 - [6] Y. Nara, H. Niemi, A. Ohnishi and H. Stcker, Phys. Rev. C **94**, no. 3, 034906 (2016)
 - [7] J. Adam *et al.* [STAR Collaboration], arXiv:1905.02052 [nucl-ex].
 - [8] S. Chatterjee and P. Boek, Phys. Rev. Lett. **120**, no. 19, 192301 (2018)
 - [9] X. Dong and V. Greco, Prog. Part. Nucl. Phys. **104**, 97 (2019)
 - [10] T. Matsui and H. Satz, Phys. Lett. B **178**, 416 (1986)
 - [11] L. Grandchamp, R. Rapp and G. E. Brown, Phys. Rev. Lett. **92**, 212301 (2004)
 - [12] X. Zhao and R. Rapp, Phys. Lett. B **664**, 253 (2008)
 - [13] X. l. Zhu, P. f. Zhuang and N. Xu, Phys. Lett. B **607**, 107 (2005)
 - [14] L. Yan, P. Zhuang and N. Xu, Phys. Rev. Lett. **97**, 232301 (2006)
 - [15] X. Yao and T. Mehen, Phys. Rev. D **99**, no. 9, 096028 (2019)
 - [16] G. Bhanot and M. E. Peskin, Nucl. Phys. B **156**, 391 (1979).
 - [17] H. Satz, J. Phys. G **32**, R25 (2006)
 - [18] B. Chen, Chinese Physics C Vol.43, No.12 (2019) 124101.
 - [19] A. Andronic, P. Braun-Munzinger, K. Redlich and J. Stachel, Nucl. Phys. A **789**, 334 (2007)
 - [20] X. Yao and B. Mller, Phys. Rev. D **100**, no. 1, 014008 (2019)
 - [21] W. Shi, W. Zha and B. Chen, Phys. Lett. B **777**, 399 (2018)
 - [22] Y. p. Liu, Z. Qu, N. Xu and P. f. Zhuang, Phys. Lett. B **678**, 72 (2009)
 - [23] X. Du and R. Rapp, Nucl. Phys. A **943**, 147 (2015)
 - [24] J. P. Lansberg and H. S. Shao, Eur. Phys. J. C **77**, no. 1, 1 (2017)
 - [25] A. Kusina, J. P. Lansberg, I. Schienbein and H. S. Shao, Phys. Rev. Lett. **121**, no. 5, 052004 (2018)
 - [26] V. Emel'yanov, A. Khodinov, S. R. Klein and R. Vogt, Phys. Rev. C **61**, 044904 (2000)
 - [27] V. Emel'yanov, A. Khodinov, S. R. Klein and R. Vogt, Phys. Rev. C **59**, 1860 (1999)
 - [28] D. C. McGlinchey, A. D. Frawley and R. Vogt, Phys. Rev. C **87**, no. 5, 054910 (2013)
 - [29] B. Chen, T. Guo, Y. Liu and P. Zhuang, Phys. Lett. B **765**, 323 (2017)
 - [30] K. J. Eskola, H. Paukkunen and C. A. Salgado, JHEP **0904**, 065 (2009)
 - [31] B. Chen, Phys. Rev. C **93**, no. 5, 054905 (2016)
 - [32] A. Adare *et al.* [PHENIX Collaboration], Phys. Rev. Lett. **98**, 232002 (2007)
 - [33] B. Schenke, S. Jeon and C. Gale, Phys. Rev. C **82**, 014903 (2010)
 - [34] B. Schenke, S. Jeon and C. Gale, Phys. Rev. Lett. **106**, 042301 (2011)
 - [35] P. Huovinen and P. Petreczky, Nucl. Phys. A **837**, 26 (2010)
 - [36] K. Zhou, N. Xu, Z. Xu and P. Zhuang, Phys. Rev. C **89**, no. 5, 054911 (2014)
 - [37] B. I. Abelev *et al.* [STAR Collaboration], Phys. Rev. Lett. **101**, 252301 (2008)